JOURNAL OF MATERIALS SCIENCE 5 (1970) 557-565

Crystallisation of Lithium Zinc Silicates

Part 1 *Phase Equilibria in the System Li_4SiO_4-Zn_2SiO_4*

A. R. WEST, F. P. GLASSER
Department of Chemistry, University of Aberdeen, Old Aberdeen, Scotland

Phase relations on the Li_4SiO_4-Zn_2SiO_4 join of the Li_2O-ZnO-SiO_2 system have been studied. Extensive ranges of solid solutions form, and many of these have structures which are related to those of Li_3PO_4; the mechanism of lithium $\rightleftharpoons$ zinc replacement is discussed. Ten binary phases have been found; seven probably occur at equilibrium. In addition, the high-temperature polymorphism of Li_4SiO_4 has been studied. Physical data are presented to characterise the thermodynamically stable phases, and their stability relations depicted on a temperature-composition equilibrium diagram.

1. Introduction

Phase relations in the Li_2O-ZnO-SiO_2 system have been studied previously [1, 2] because some compositions within this system may yield useful glass-ceramics. In a wide range of ternary compositions, an orthosilicate phase, or phases, co-exist with SiO_2 at subsolidus temperatures. Orthosilicates may, therefore, occur as crystallisation products of glasses, including those relatively rich in silica. Stewart and Buchi described two orthosilicates to which they assigned the formulae Li_2ZnSiO_4 and $Li_8Zn_{10}Si_7O_{28}$. Lam fixed the composition of the more zinc-rich phase at $Li_4Zn_4Si_3O_{12}$, but also noted that both phases had a range of composition extending along the orthosilicate join. At 900° C, he fixed the limits of solid solution at *ca.* 5 mole %* excess Zn_2SiO_4 in the Li_2ZnSiO_4 phase, and at *ca.* 62 to 72% Zn_2SiO_4 for the $Li_4Zn_4Si_3O_{12}$ phase. Initially, we studied the crystallisation of some glasses in the silica-rich portion of this system, but were unable to identify some of the orthosilicates using the published data. This led to a more thorough study of the orthosilicate join. Part 1 describes the thermodynamically stable phase relations; however, metastable phase assemblages were frequently encountered and these are described in Part 2.

2. Experimental

The starting materials for preparation of Li_4SiO_4-Zn_2SiO_4 compositions were a chemically pure grade of Li_2CO_3, "Analar" ZnO and very pure crushed quartz crystal, supplied by Thermal Syndicate Ltd. Compositions containing 45 to 100% Zn_2SiO_4 were prepared in *ca.* 10 to 15 g amounts by heating appropriate mixtures. These were blended in an agate mortar as an ethanol-containing slurry for approximately 10 min, dried gently, and fired in an electric furnace. Platinum crucibles were used for firing; it was necessary to fire each composition four or five times, with intermediate regrinding, in order to produce a homogeneous sinter and without also encountering excessive loss of lithium oxide. The firings were generally started at *ca.* 800° C and the last firing finished at *ca.* 1280° C. Compositions containing 5 to 45% Zn_2SiO_4 could be prepared most rapidly by reacting the appropriate quantities of Li_4SiO_4 and Zn_2SiO_4. Compositions from Li_4SiO_4 up to ~ 45% Zn_2SiO_4 were found to react with platinum; because they also have low solidus temperatures, they were put in gold foil envelopes and sintered at temperatures not exceeding 950° C.

Solidus and liquidus temperatures were determined by the quenching technique; phases present in the quenched runs were identified by their powder X-ray patterns or by petrographic microscopy. It was not feasible to use high temperature microscopy for a direct study of the melting relationships because of excessive lithium loss. Weight loss experiments on samples of approximately 1 g and containing 50% Zn_2SiO_4

*All percentages in this paper are in mole%.

TABLE I A. X-ray powder diffraction data for lithium-zinc orthosilicates

γ_{II} d (Å)	I	γ_I d (Å)	I	γ_0 d (Å)	I	*hkl*	β_{II} d (Å)	I	*hkl*	β_I d (Å)	I	*hkl*	C d (Å)	I	*hkl*
		5.50	40	5.50	60	110				5.48	60	110	8.25	40	110
5.50	10	5.40	10	5.40	10	020	5.50	10	010	5.45	10	020	6.50	40	200
4.60	10	4.60	10	4.60	10	011	4.15	60	110	4.09	40	120	5.60	10	210
4.14	80	4.09	80	4.09	80	120	3.99	60	101	3.93	40	101	5.50	80	
4.02	60	3.97	80	3.99	40	101				3.68	100	111	5.30	10	020
				3.97	60		3.70	20	011	3.66	20	021	4.60	10	011
3.73	20	3.71	60	3.71	20	111, 021	3.21	40	200, 111	3.16	20	200, 121	4.42	20	111
				3.69	100					3.11	60	130	4.12	80	220
3.21	20	3.18	20	3.19	20	200, 121	2.76	80	210	2.71	80	220	4.04	40	
				3.17	10		2.70	100	020	2.67	60	040	3.99	60	201
		3.12	20	3.12	40	130, 210	2.52	80	002	2.49	100	002	3.74	40	211
2.94	20	2.93	20	2.93	10	031	2.42	80	211	2.38	60	221	3.70	100	
				2.92	20		2.38	40	021	2.35	40	041			
2.75	100	2.71	100	2.74	60	220							3.29	40	400
				2.71	80								3.21	10	221
2.69	80	2.68	80	2.68	80	040							3.18	20	410
2.66	20	2.65	40	2.65	40	131							3.12	60	311, 230
				2.64	10								3.11		
2.63	40	2.58	40	2.60	10	211							2.92	20	031
				2.58	40								2.89	20	
2.56	100	2.535	100	2.54	80	002							2.78	60	420
				2.52	60								2.72	60	
													2.67	60	040
													2.63	60	
													2.65	20	411
													2.61	10	231
													2.59	10	
													2.53	80	002
(a, b)		(a, c)		(a, c, e)			(d, b)			(d, c)			(f, c, e)		

Notes:
a. solid solution composition 75% Li_4SiO_4-25% Zn_2SiO_4; b. data obtained at 700° C; c. data obtained at 25° C; d. solid solution composition: 50% Li_4SiO_4-50% Zn_2SiO_4; e. indexed on the basis of pseudo symmetry; f. solid solution composition, 38% Li_4SiO_4-62% Zn_2SiO_4.

TABLE I B. X-ray diffraction data for lithium-zinc orthosilicates: unit cells and probable space groups. Densities

Phase	Symmetry	a (Å)	b (Å)	c (Å)	Space group	Density (g cc^{-1}) 25° C
γ_{II} (25% Zn_2SiO_4, 700° C)	orthorhombic	6.42	10.76	5.12	$Pmnb - D_{2h}^{16}$	
γ_I (25% Zn_2SiO_4, 25° C)	orthorhombic	6.36	10.72	5.07		3.62_5*
γ_0 (25% Zn_2SiO_4, 25° C)	pseudo-orthorhombic (monoclinic)	6.36	10.72	5.06		3.35†
β_{II} (50% Zn_2SiO_4, 700° C)	orthorhombic	6.42	5.40	5.04	$Pmn2_1 - C_{2v}^7$	
β_I (50% Zn_2SiO_4, 25° C)	orthorhombic	6.32	10.68	4.98		3.37_3
C (62% Zn_2SiO_4, 25° C)	pseudo-orthorhombic	13.16	10.6	5.06		3.64_3*
Low – Li_4SiO_4 (25° C)	monoclinic: $\beta = 89.5°$	5.14	6.10	5.30	$P2_1/m - C_{2h}^2$	
High – Li_4SiO_4 (800° C)	pseudo-orthorhombic	5.30	6.32	5.45		

* Density for 66.7% Zn_2SiO_4 composition. † Density for 50% Zn_2SiO_4 composition.

showed that at 1350° C, loss of lithium did not exceed 1 to 2% "Li_4SiO_4" in runs of 2 to 3 h duration. However, at the lithium-rich end of the system, lithia losses increased rapidly and only at subsolidus temperatures was it possible to study phase relations quantitatively.

X-ray powder diffraction patterns were recorded at ambient temperatures using either a Nonius Guinier camera or a Philips PW 1051 diffractometer and at elevated temperatures, with a Nonius Guinier-Lenne camera. In the high-temperature X-ray camera (HTXR), the samples were supported on a metal gauze made of platinum or, for high-lithia compositions, stainless steel. The latter remained unattacked in a flowing nitrogen atmosphere below 900° C. Powder X-ray lines from the gauze could be used as an internal standard to calibrate d-spacings; temperatures were measured with a Pt-10% Rh/Pt thermocouple fixed in the platinum-alloy sample holder frame. DTA runs were made on a Du Pont 900 instrument, usually at a fixed

TABLE II Solidus and liquidus data for Li_4SiO_4-Zn_2SiO_4 compositions

Composition (mole % Zn_2SiO_4)	Temperature (° C)	Time (minutes)	Phases present
50	1494	30	liquid
50	1451	10	γ_{II}
62.5	1440	20	liquid
62.5	1420	10	liquid + γ_{II}
62.5	1372	10	γ_{II}
75	1354	40	liquid + γ_{II}
75	1316	30	γ_{II}
85	1365	15	liquid
85	1339	15	liquid + γ_{II}
85	1305	10	γ_{II} + willemite
90	1413	30	liquid + willemite

heating or cooling rate of 20° C min^{-1}. Both the DTA and the HTXR camera gave a *continuous* record with changing temperature and therefore, polymorphic transformations could be followed directly by these two complementary techniques. Densities of crystalline phases were determined using a Beckmann model 930 gas comparison pycnometer; 25 g samples were specially prepared for these determinations and ten separate density measurements made on each sample.

3. Results and Discussion

3.1. The Phase Equilibria

In addition to the end members, α-Zn_2SiO_4 and the polymorphs of Li_4SiO_4, ten binary phases were encountered: however, only seven of these have a range of true thermodynamic stability. All the phases have considerable structural similarity to each other, and in most instances, form extensive solid solutions. Only three of the phases can be obtained at equilibrium at ambient temperatures, therefore, some of the X-ray data which were used to characterise these phases had, of necessity, to be recorded at higher temperatures. Full powder X-ray data will be submitted to the ASTM, but sufficient data to identify the stable phases are shown in table I: part A shows powder data, and part B summarises other crystallographic data and observed densities. In order to facilitate comparison, the powder data shown were recorded at only two temperatures: ambient and 700° C, and for the minimum number of different compositions. Representative solidus and liquidus temperatures that were located by quenching runs are shown in table II. Orthosilicate liquids do not quench to yield a glass; therefore the presence of a former liquid phase in quenched runs must be inferred from textural evidence: the crystalline phase or phases which are believed to have been present as the primary phase are shown. The position of phase boundaries at subsolidus temperatures had to be located by both dynamic and static methods. Critical determinations which rest on HTXR and DTA are shown in table III; those determined by static heating, followed by cooling at various rates, are shown in table IV.

These representative data may be combined with the results of numerous other experiments to give the equilibrium diagram, fig. 1. The Li_2ZnSiO_4 composition melts congruently at 1472 ± 20° C; this compares with Lam's value of 1480 ± 4° C from DTA. Between Li_2ZnSiO_4 and Zn_2SiO_4, liquidus temperatures drop to a eutectic located at 84 ± 4% Zn_2SiO_4 and 1340 ± 20° C. Liquidus relations are not known on the high Li_2O side, but the minimum solidus temperature is probably lower, of the order of 1050° C. A large endotherm appears at *ca.* 1050° C in the DTA upon heating compositions containing 15 to 20% Zn_2SiO_4. Only the initial drop in melting temperature from Li_2ZnSiO_4 has been confirmed by quenching; the probable incongruent melting of Li_4SiO_4 described previously [3] has been indicated by dashed lines. However, it is the subsolidus relations which are of most interest. Only α-Zn_2SiO_4 (willemite) appears as a phase of essentially constant composition, containing < 1% Li_4SiO_4 at all temperatures. On the other hand, Li_4SiO_4 and the binary phases have compositions which are variable over wide limits.

Li_4SiO_4 is capable of taking ~ 18% Zn_2SiO_4 into solid solution at the highest temperatures studied, *ca.* 900 to 950° C. Li_4SiO_4 itself is thermally active and gives three small reversible DTA effects at temperatures of 608, 666 and 724° C. HTXR detected only one, probably higher-order, crystallographic transformation: this corresponds most closely to the DTA effect at 666° C. The HTXR shows that in the tem-

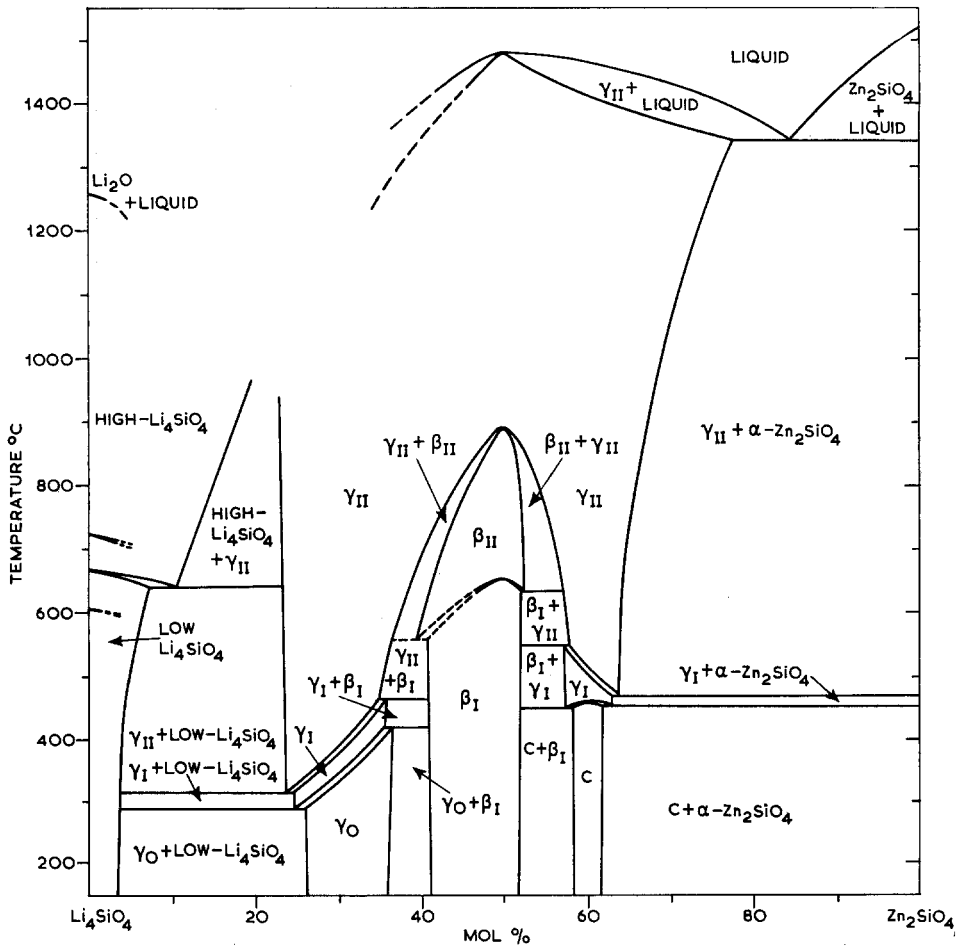

Figure 1 Phase equilibrium diagram for the system Li_4SiO_4-Zn_2SiO_4. See text for fuller discussion of the nomenclature and of those two-phase regions which are not marked with the phases present.

perature range 600 to 750° C, the relative intensities of many powder X-ray reflections alter markedly: moreover, the variation in *d*-spacing with temperature also changes more markedly in this range. It was not possible to decide if one or more minor, first-order transformations were superimposed on these higher-order effects. Upon addition of a few % Zn_2SiO_4 the situation becomes simpler: the upper and lower inversions disappear. The remaining inversion can be followed by both DTA and HTXR through a range of zinc-containing Li_4SiO_4 solid solutions. It remains reversible at 5% Zn_2SiO_4, but becomes more diffuse at higher zinc contents; the inversion temperature falls gradually with increasing zinc content of the solid solutions. The two heat effects which disappear upon adding zinc are shown as dashed lines extending a short distance on the diagram, indicating that the mode of their disappearance is unknown. A range of Li_4SiO_4 solid solutions are shown as decomposing by peritectoid reaction at ~ 640° C. These solid solutions, containing > 10% Zn_2SiO_4, can be preserved by rapid quenching to room temperature as the high form of Li_4SiO_4 or as a form which closely resembles it.

The Li_4SiO_4 solid solutions are separated from the more zinc-rich γ- and β-solid solutions by a series of two-phase regions. The length of tie lines across these regions tends to decrease with increasing temperature, but no evidence has been found for the existence of a continuous range of solid solutions at temperature as high as ~ 950° C. Solidus temperatures, estimated from DTA, are ~ 1050° C so that it is possible that the two-phase region might close over for a small range of temperatures below the solidus.

The central portion of the diagram is domi-

TABLE III Subsolidus phase transformations in Li_4SiO_4-Zn_2SiO_4; results determined by dynamic methods

Composition (mole % Zn_2SiO_4)	Method	Reaction	Temperature (° C)
71.5	HTXR	$\gamma_{II} + Zn_2SiO_4 \rightleftarrows \gamma_{II}$	1050 – 1100° C
62.5	DTA, HTXR	$C \rightleftharpoons \gamma_I$	451
62.5	DTA, HTXR	$\gamma_I \rightleftharpoons \gamma_{II}$	473
55	HTXR	$\beta_{II} \rightleftharpoons \gamma_{II}$	800
50	DTA	$\beta_I \rightleftharpoons \beta_{II}$	649
50	HTXR	$\beta_{II} \rightleftharpoons \gamma_{II}$	870*
45	DTA	$\beta_I \rightleftharpoons \beta_{II}$	638
45	HTXR	$\beta_{II} \rightleftharpoons \gamma_{II}$	780
33	HTXR	$\gamma_0 \rightleftharpoons \gamma_I$	350 ± 50
33	HTXR	$\gamma_I \rightleftharpoons \gamma_{II}$	430 ± 30
25	HTXR	$\gamma_0 \rightleftharpoons \gamma_I$	275 ± 30
25	HTXR	$\gamma_I \rightleftharpoons \gamma_{II}$	320 ± 20
0	DTA	low $\rightleftharpoons \rightleftharpoons \rightleftharpoons$ high Li_4SiO_4	608 666 724

* By DTA, superheating of β_{II} occurred, giving the inversion temperature as 915° C.

TABLE IV Subsolidus data for Li_4SiO_4-Zn_2SiO_4 compositions: results obtained from static heating experiments

Composition (mole % Zn_2SiO_4)	Temperature (° C)	Time	Cooling rate	Phases present at room temperature
85	1305	10 min	quench	$C' + Zn_2SiO_4$*
75	1316	30 min	quench	C'
71.5	1150	5 d	quench	$C' + \gamma_I$
71.5	1040	8 h	quench	γ_I, trace Zn_2SiO_4
66	700	14 d	quench	γ_I, trace Zn_2SiO_4
62.5	700	14 d	slow (30 min)	C
55	680	3 d	slow (30 min)	$\beta_I + C$
50	680	3 d	slow (30 min)	β_I
40	580	10 d	slow (30 min)	$\beta_I + \gamma_0$
33	500	4 d	slow (30 min)	γ_0
33	950	2 h	quench	γ_I
25	950	30 min	quench	γ_{II}
21.5	950	2 h	quench	γ_{II} + high Li_4SiO_4
21.5	800	4 h	very slow (~ 2 d)	γ_0 + low Li_4SiO_4
5.5	950	2 h	quench	low Li_4SiO_4
5.5	800	2 h	very slow (~ 2 d)†; reheat to 400° C and cool slowly (~ 2 h)	γ_0 + low Li_4SiO_4

* C′ is a metastable phase and will be dealt with in Part II.
† On slow cooling a metastable phase designated "D" appeared, which disappeared on reheating. It will be dealt with in more detail in Part II.

nated by two ranges of solid solutions, designated as the γ- and β-phases. The nomenclature is designed to suggest that close structural relations exist within any one family: Thus the γ-family has three structurally similar polymorphs. These are designated γ_{II}, γ_I and γ_0. Polymorphs in any one family are not only structurally similar but transform to each other reversibly, the inversions being relatively rapid and presumably of the displacive type. Although the γ_{II} field extends across half the width of the diagram at solidus temperatures, it is only at the high-lithia end that its solid solutions can be quenched to ambient. It was found that γ_I-solid solution could be quenched towards both limits of its compositional extent; once at about 35% and again at about 60% Zn_2SiO_4. Intermediate compositions always inverted upon quenching to yield γ_0-solid solutions at ambient. The transformations: $\gamma_0 \rightleftharpoons \gamma_I \rightleftharpoons \gamma_{II}$ could, however, be followed reversibly by HTXR; at 25 to 30% Zn_2SiO_4, these inversions occur too slowly to be followed reversibly by DTA.

At zinc contents close to the Li_2Zn (1:1) ratio, and at temperatures below ~ 870° C, the γ-family phases are interrupted by the appearance of the β-family phases. These β-phases have the ideal composition Li_2ZnSiO_4 and in general, exhibit a much more limited compositional range of single-phase formation than the

γ-family phases. The ideal composition of the β-phase is indicated by the very pronounced thermal stability maximum of β at the 1:1 composition. At this ratio, γ_{II} solid solutions convert completely to the β_{II}-phase in a few hours at 650° C. In compositions close to the 1:1 ratio the equilibrium $\gamma_{II} \rightleftharpoons \beta_{II}$ is readily reversible in static heating experiments. However, over a wide range of cooling rates varying from 20° C min^{-1}, as used in DTA, to much faster quenching, a γ_{II} solid solution having the 1:1 ratio is preserved to ambient as a γ_0 solid solution; no conversion to the β-phase will occur owing to the comparative sluggishness of the reaction. The equilibrium conversion between γ- and β-type phases has, however, been followed to temperatures as low as *ca.* 450° C, although at these temperatures equilibrium is achieved only in static runs of several days duration. The range of β-solid solutions extends from the 1:1 composition to approximately 52% Zn_2SiO_4: however, the maximum solid solution of Li_4SiO_4 is somewhat larger, *ca.* 10% at ~ 650° C. The conversion of γ- to β-solid solutions becomes very sluggish at higher lithium contents, hence it is more difficult to fix the exact limits of solid solution on the lithia-rich side than on the zinc-rich side of the Li_2ZnSiO_4 composition. The $\beta_I \rightleftharpoons \beta_{II}$ inversion temperature, whose intersection with the limiting two phase gaps marks the maximum limit of solid solutions, passes through a thermal maximum at 649° C at the 1:1 composition. The inversion gives rise to a fairly small broad DTA signal at this composition: in the Li-rich solid solutions, the inversion temperature falls but it was not possible to measure exactly the drop in inversion temperature, owing in part to the difficulty of preparing homogeneous lithium rich β-solid solutions, and in part, to the complex nature of the inversion.

High temperature X-ray patterns combined with X-ray data obtained from quenched samples, show that both the β_I- and β_{II}-phases exist in two modifications at the 1:1 ratio: the second modifications have been designated β_I' and β_{II}' respectively. The distinction is shown graphically in fig. 2, which compares the appearance of the diffraction patterns of the β-family phases. The relative stability of the β-phases having the 1:1 composition is shown in fig. 3. Cooling of β_{II} yields β_{II}' over a short range of temperatures. The reaction $\beta_{II} \rightleftharpoons \beta_{II}'$ appears to be rapidly reversible at ~ 670° C and can be followed in the high temperature X-ray photographs. The heat effect associated with the reaction is apparently too small to be detected by DTA. Fig. 1 should probably be modified to include a small field for β_{II}' which, at the 1:1 composition, extends from 650 to ~ 670° C. However, because its extension through the range of compositions which form the β-phase has not been detected, the β_{II} field has not been subdivided.

If a small sample of β_{II} is removed from the furnace and allowed to cool in air from temperatures above 675° C, it converts to β_I', but with rapid quenching, β_{II}' is obtained. Upon prolonged annealing of samples containing β_I' at

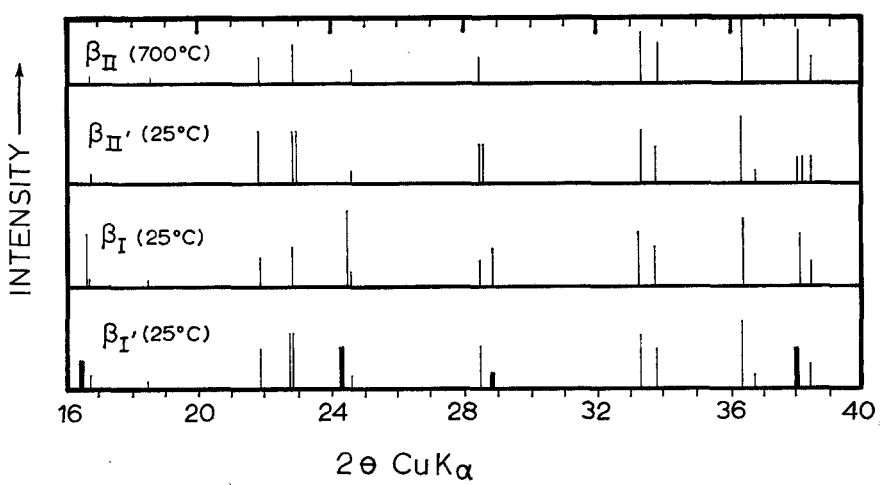

Figure 2 Powder X-ray diffraction data for the four β-family modifications. Data are for the composition Li_2ZnSiO_4. Complete powder data for the β_I- and β_{II}-phases are collected in table I.

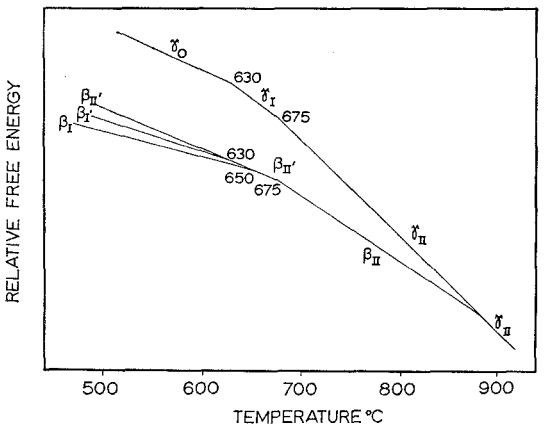

Figure 3 Stability of the various polymorphs of lithium zinc silicate having the composition Li_2ZnSiO_4. Absolute values of the free energies are not known, and any curvature of the free energy vs temperature curves has been neglected. The most stable phase is that which, at some fixed temperature, has the lowest free energy. See text for a discussion of the metastable paths.

300 to 400° C the β_I'-phase is converted entirely to β_I. Using HTXR, with a heating rate of $\sim 1°$ C min^{-1}, β_I' reverts to β_I at *ca.* 400° C. With the faster DTA heating rates, β_I' can be retained to much higher temperatures and reverts to β_I giving a broad exotherm at $\sim$ 630° C. This exotherm is superimposed on the broad $\beta_I \rightarrow \beta_{II}' \rightarrow \beta_{II}$ endotherm, at approximately 650° C. These experiments have been used to infer the relative order of thermodynamic stability of the various phases having the 1:1 composition, as shown in fig. 3. Thus, the β_I'-phase is probably metastable at all temperatures. It is noteworthy that for this composition, by selecting appropriate cooling conditions, four crystalline phases namely: β_I, β_I', β_{II}' and γ_0 may be obtained at ambient temperatures, either as single phases or as mixtures.

At $\sim$ 60% Zn_2SiO_4, cooling of γ_{II}-solid solution again produces a field of stability for the γ_I-solid solution. The $\gamma_I \rightleftharpoons \gamma_{II}$ inversion, also encountered in a range of higher-Li compositions, is thus effectively interrupted across an intermediate range of compositions by the appearance of the β-family of phases. However, the zinc-rich γ_I-solid solutions do not transform to a γ_0-solid solution upon further cooling, but instead give rise to another new phase, designated phase C. The temperature of the C $\rightleftharpoons \gamma_I$ transformation varies only slightly over the limited range of compositions in which C was found to occur at equilibrium: however, the transformation does appear to pass through a thermal maximum located at 452° C and 60% Zn_2SiO_4. The C-phase probably has the ideal formula $Li_8Zn_6Si_5O_{20}$ or $Li_6Zn_5Si_4O_{16}$. It can be considered as pseudo-orthorhombic, although its true symmetry is less than orthorhombic. Its pseudo-orthorhombic cell is derived from that of γ_I by doubling the *a*-axis. Phase C-, γ_I- and γ_{II}-solid solutions each co-exist with Zn_2SiO_4 over appropriate temperature intervals; the compositions of co-existing phases are sufficiently different to give rise to broad two-phase regions. The univariant curve marking the limit of γ_{II}-solid solution extends toward Zn_2SiO_4 with increasing temperature: its position can be followed either directly by HTXR, especially above *ca.* 900° C, or indirectly, by static heating, quenching, and examination of the products at ambient temperature.

3.2. Powder X-ray Data

Among the evidence for the existence of a wide range of solid solutions, the systematic variation in X-ray *d*-spacings of an individual phase as a function of composition may be cited. Fig. 4 shows data for the γ_{II}-phase, which forms the most extensive range of solid solutions. These data were obtained at 700 $\pm$ 10° C, the lowest temperature at which it is possible to maintain a wide, uninterrupted range of γ_{II}-solid solutions for sufficient time to obtain a powder pattern. The solid solutions are orthorhombic, therefore the variation in position of the reflections (200), (040) and (002) define the change in unit cell volume. The *c* cell dimension does not vary appreciably with changing composition, but both *a*- and *b*-axes undergo a marked change in slope at the 1:1 ratio, again indicating the special nature of this composition. The calculated cell volume (V) has its *minimum* value (349.4 Å^3) at the 1:1 composition: V increases linearly upon shifting to either zinc-rich or lithium-rich compositions. At 75% Zn_2SiO_4, V = 351.4 Å^3; at 25% Zn_2SiO_4, V = 350.8 Å^3.

These results obtained at 700° C are, after allowing for the effects of thermal expansion, identical with those obtained at higher and lower temperatures inasmuch as they show a marked change in axial ratios in compositions lying to the zinc-rich side of the 1:1 ratio.

From a comparison of powder X-ray data and experimental conditions used, it is believed that Stewart and Buchi obtained the γ_0-phase of the 1:1 composition (which they identified as

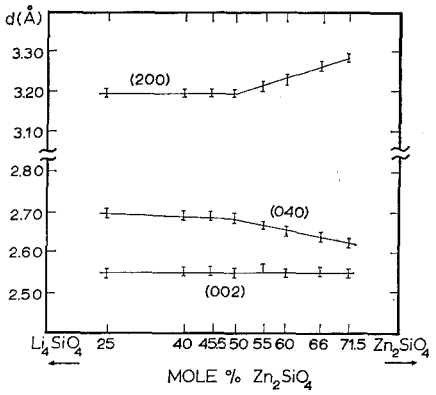

Figure 4 Variation in the *a*, *b*, and *c* unit cell dimensions of the γ_{II} lithium zinc silicates as a function of composition, at 700° C.

"Li_2O . ZnO . SiO_2") and also at higher zinc contents, a mixture of willemite and phase C which they identified as "$4Li_2O.10ZnO.7SiO_2$". The first of these phases may have this composition, but would be metastable with respect to a β_I-solid solution at ambient; in the second case, the C-phase is presumed to have been formed by the comparatively rapid inversion of an undercooled γ_{II}-solid solution. Thus, their experimental observations are basically in agreement with ours, although they greatly oversimplify the sequence of compound formation and phase changes which may occur in this system. It should be noted that the stable relations in this system are complicated by the appearance of additional non-equilibrium phases; these will be described separately. However, the phase diagram presented here and a knowledge of the kinetics of the inversions, are sufficient to account for the phases described by Stewart and Buchi.

3.3. Crystal Chemistry of the Lithium Zinc Silicates

Comparison of the X-ray powder data show that the γ_{II}-phase is isostructural with the high-temperature form of Li_3PO_4, and that the β_{II}-phase is isostructural with the low-temperature form of Li_3PO_4. Thus, the substitution which occurs is ideally:

$$(Li_{2\cdot0}^{+}\,Li_{1\cdot0}^{+}) + P^{5+} = (Li_{2\cdot0}^{+}\,Zn_{1\cdot0}^{2+}) + Si^{4+}.$$

Advantage has been taken of this isomorphous relationship to index the powder data by analogy with Li_3PO_4. It is interesting to note that the powder data for the lithium zinc silicates may be indexed in other ways: for example, Stewart and Buchi, using trial and error methods found large tetragonal cells which apparently fitted the powder data. However, an olivine-type cell provides a much better fit to the powder data; $\gamma_{II}Li_2ZnSiO_4$ has the correct silicon to oxygen ratio, orthorhombic symmetry, and unit cell dimensions to be an olivine. Indeed, its isomorph, Li_3PO_4, was once classified as an olivine on the basis of its cell dimensions and space group.* However, the crystal structure of high Li_3PO_4 has been studied [5]; it has an hexagonal close-packed oxygen arrangement like that of an olivine, but the lithium ions are all packed into approximately tetrahedral sites, rather than into octahedral sites. The crystal structure of low Li_3PO_4 is very similar to that of the high form [6].

The crystal chemistry of the lithium zinc silicates does differ in several important respects from that of Li_3PO_4. First, the orthorhombic symmetry present in either form of Li_3PO_4 may not be preserved to ambient temperature in Li_2ZnSiO_4. Thus, at this composition, $\gamma_{II}Li_2ZnSiO_4$ could not be obtained in the orthorhombic form at ambient temperatures: instead it underwent two rapid inversions, the first of which generated an extra set of reflections in the powder patterns, and the second, which introduced a minor structural distortion that was indicated by a slight splitting of some of the powder X-ray lines. The symmetry of the low form is thus probably monoclinic; because of the strong pseudo-orthorhombic symmetry, and because the exact symmetry is unknown, orthorhombic indices have been retained for present purposes. Retaining the orthorhombic indices also helps show the close structural similarity between the γ_{II}-, γ_I- and γ_0-phases. This progressive increase in structural complexity with decreasing temperature is also apparent in the β-family; the β_{II}-phase undergoes a rapid inversion upon cooling which results in a doubling of the *b*-axis to give β_I. A second difference between Li_3PO_4 and the lithium zinc silicates is that in the former, all the larger tetrahedral holes are occupied by only one type of cation (Li^+), whereas in the latter, these sites are occupied by both Li^+ and Zn^{2+}. The large extent of solid solution between two orthosilicates containing cations of different charge was an unexpected

* More recently, the mineral lithiophosphate, Li_3PO_4, has also been classified as an olivine on the basis of its cell dimensions and powder X-ray pattern by Fischer [4]. However, its published powder data appear to be identical with that of synthetic, low Li_3PO_4. Pending further study, its classification as an olivine is therefore suspect.

feature of the equilibrium relationships; in systems which might be expected to serve as models: e.g. Na_4SiO_4-Ca_2SiO_4, little if any solid solution occurs.

If the γ_{II}-phase is a structural derivative of high-Li_3PO_4, the existence of a range of solid solutions may be explained as follows. Li_3PO_4 is known to contain two types of non-equivalent lithium sites. In each unit cell, there are eight Li sites which provide a fairly regular tetrahedral oxygen environment (M_1) and four Li sites which provide a rather less regular tetrahedral environment (M_2). It seems reasonable to conclude that at the Li_2Zn (1:1) ratio, the M_1 sites are fully occupied by Li^+ and the M_2 sites by Zn^{2+}. From this composition solid solution proceeds towards Zn_2SiO_4 by replacement of lithium on M_1 sites by zinc, with concomitant production of vacant M_1 sites. Thus the solid solutions range toward the observed zinc-rich composition limit ($\sim$ 75% Zn_2SiO_4) as follows:

M_1	M_2	
(Li_8)	(Zn_4)	Si_4O_{16}
$(\square_2Zn_2Li_4)$	(Zn_4)	Si_4O_{16}

where $\square$ indicates tetrahedral-site cation vacancies. These vacancies are envisioned as being randomly distributed amongst M_1 sites in the γ_{II}-phase. The solid solutions also proceed from the Li_2Zn ratio to the limit of Li-rich compositions ($\sim$ 25% Zn_2SiO_4) as follows:

	M_1	M_2	
	(Li_8)	(Zn_4)	Si_4O_{16}
$\textcircled{Li}_2$	Li_8	(Zn_2Li_2)	Si_4O_{16}

where O denotes otherwise vacant sites (whose co-ordination is unknown) which must be occupied by Li in order to balance the electrostatic charge as more lithium substitutes for zinc on M_2 sites. The possibility of making extra sites available for lithium stuffing may be demonstrated by examining the crystal structure of Li_4SiO_4 [7] in which the oxygen packing is similar to that of Li_3PO_4-type structures; in monoclinic Li_4SiO_4, Li occupies not only tetrahedral sites, but also spills over into sites which afford 5- and 6-co-ordination. Li_4SiO_4 may thus be regarded as an "overstuffed" end member.

The fields of the various solid solutions shown in fig. 1 are separated by two-phase gaps of variable width. At one extreme, Zn_2SiO_4 (willemite) is separated from the fields of γ_{II}-, γ_I- and C-phases by two-phase regions whose width is on the order of 20 to 40%; at the other extreme, some two-phase regions were too narrow to be detected. For example, even continuous HTXR photographs have failed to record definite two-phase regions of (γ_{II} + γ_I) – solid solutions: on DTA this transformation is observed as a sharp, essentially isothermal phase change across a wide range of solid solution compositions. In fig. 1, those two phase regions whose extent could be measured directly are labelled to show co-existing phases; unlabelled two-phase regions are those which are demanded by theory, but whose existence was not detected experimentally. The width of the two-phase gaps in this system seems to be directly proportional to the structural differences between the co-existing phases: unfortunately the relationship cannot be made more exact because of the difficulty of defining "structural differences" quantitatively.

Acknowledgement

One of us (A.R.W.) has been supported by a University studentship from the Robbie, Japp and Coutts Funds. The Science Research Council has provided funds for equipment and materials.

References

1. I. M. STEWART and G. J. P. BUCHI, *Trans. Brit. Ceram. Soc.* **61** (1962) 615.
2. A. H. LAM, Ph.D. Thesis, University of Sheffield (1964).
3. F. C. KRACEK, *J. Phys. Chem.* **34** (1930) 2645.
4. D. J. FISCHER, *Amer. Miner.* **43** (1958) 761.
5. J. ZEEMANN, *Acta Cryst.* **13** (1960) 863.
6. C. KEFFER, A. MIGHELL, F. MAUER, H. SWANSON, and S. BLOCK, *Inorg. Chem.* **6** (1967) 119.
7. H. VOLLENKLE, A. WITTMANN, and H. NOWOTNY, *Monat. Chem.* **99** (1968) 1360.

Received 3 February and accepted 25 March 1970.